

Thermal fixing of holographic gratings in planar LiNbO₃:Ti:Fe waveguides

J. Hukriede, D. Kip, E. Krätzig

Universität Osnabrück, Fachbereich Physik, D-49069 Osnabrück, Germany
 (Fax: +49-541/969-2670)

Received: 21. July 1997/Revised version: 13 October 1997

Abstract. Refractive index gratings in planar LiNbO₃:Ti:Fe waveguides are thermally fixed during hologram recording at elevated temperatures. Different guides are fabricated by titanium indiffusion using iron-doped and nominally pure y-cut LiNbO₃ substrates and characterization is performed by dark-mode spectroscopy. The refractive index modulation of gratings written and simultaneously fixed at 180 °C is investigated as a function of propagation depth, titanium and iron concentration. The experimental results are compared with those obtained for unfixed holograms recorded at room temperature.

PACS: 42.70Ln; 42.82Et; 78.20-e

Holograms can be written in LiNbO₃ crystals by utilizing the photorefractive effect. When the sample is illuminated with a light interference pattern, mobile charge carriers are generated in the bright regions, and there is a buildup of space-charge fields, which modulate the refractive index of the material by means of the electrooptic effect.

However, the storage of volume-phase holograms in LiNbO₃ crystals suffers very much from destructive readout. If the sample is illuminated with light of the recording wavelength, charge carriers are excited again and reduce the modulation of the previously recorded space-charge field. To prevent this erasure effect and to preserve the original hologram, in 1971 Amodei and Staebler [1] had already developed the technique of ‘thermal fixing’ in LiNbO₃ crystals. Their experiments may be interpreted in the following way. Heating the sample to a constant temperature of around 180 °C during recording mobilises protons [2] (and perhaps other positively charged impurities, too), which compensate for the electronic space-charge field built up during the writing process. If the crystal is cooled down afterwards and illuminated homogeneously with incoherent light, modulated photocurrents, resulting from a modulation of filled and empty traps, are created and a fixed hologram that is stable, irrespective of the readout light, appears.

In this paper we investigate the process of thermal fixing in planar waveguides fabricated by titanium indiffusion

using iron-doped and nominally pure LiNbO₃ substrates. The guides are of great interest in the growing field of integrated optics. Thermally fixed sinusoidal refractive index gratings in optical waveguides enable useful applications in signal processing and beam manipulation: grating couplers allow the coupling of light through the substrate into the waveguide layer, extremely narrow bandwidth mirrors fabricated with the help of reflection holograms allow the selection of just one desired wavelength, and multiplexing/demultiplexing systems allow us to combine or separate light of different wavelengths at the input or output of an optical data transmission system.

1 Basic equations

In planar optical waveguides light can be guided by total reflection in the region of increased refractive index. When a light beam propagates along the x -direction in a y -cut sample, the distributions of electric and magnetic field can be written in the form

$$\mathbf{E}(x, y, t) = \mathbf{U}(y)e^{i(\omega t - \beta x)}, \quad (1)$$

$$\mathbf{H}(x, y, t) = \mathbf{V}(y)e^{i(\omega t - \beta x)}, \quad (2)$$

where \mathbf{U} and \mathbf{V} are the field distributions and $\beta = k_0 n_{\text{eff}}$ is the effective wave number. The wave number in free space is denoted by k_0 and the effective refractive index of a guided mode by n_{eff} . Combining Maxwell’s equations with the continuity conditions of the field distributions leads to the mode equations for TE and TM modes:

$$\partial_y^2 U_z + (k_0^2 \varepsilon_{33} - \beta^2) U_z = 0, \quad (3)$$

$$\varepsilon_{22} \partial_y (\varepsilon_{11}^{-1} \partial_y V_z) + (k_0^2 \varepsilon_{22} - \beta^2) V_z = 0. \quad (4)$$

All other components of \mathbf{U} and \mathbf{V} are zero or can be neglected. Here ε_{ii} denotes the diagonal elements of the dielectric tensor $\hat{\varepsilon}$. The modes of a waveguide differ considerably in their characteristic field distributions. For the holographic measurements described in this paper it is useful to introduce

the effective depth d_{eff} of a guided TE mode:

$$d_{\text{eff}} = \frac{\int y |U_z(y)|^2 dy}{\int |U_z(y)|^2 dy}. \quad (5)$$

An elementary sinusoidal hologram can be characterized by its diffraction efficiency η . Throughout this paper, the definition

$$\eta = \frac{I_{\text{diff}}}{I_{\text{diff}} + I_{\text{trans}}} \quad (6)$$

is used, with I_{diff} and I_{trans} as the intensities of the diffracted and the transmitted beam in the waveguide. The measurement of η using guided TE modes in y -cut waveguides allows us to calculate the spatially averaged refractive index modulation $\langle \Delta n_3 \rangle$ induced by the electrooptic effect. With the help of Kogelnik's formula [3, 4] we derive

$$\langle \Delta n_3 \rangle = \frac{\lambda \arcsin \sqrt{\eta}}{\pi s}. \quad (7)$$

The parameter s denotes the distance the TE mode has travelled through the waveguide during hologram readout and λ is the corresponding wavelength. The mean value $\langle \Delta n_3 \rangle$ is defined by

$$\langle \Delta n_3 \rangle = \frac{\int \Delta n_3(y) |U_z(y)|^2 dy}{\int |U_z(y)|^2 dy}. \quad (8)$$

2 Experimental methods

2.1 Waveguide preparation

The technique of titanium indiffusion is used to fabricate different LiNbO₃ waveguides in order to perform the measurements. Thin layers are deposited on y -cut LiNbO₃ substrates by use of an electron gun. We investigate homogeneously doped samples with an iron concentration of 674 mol ppm Fe (waveguides 1a, 1b) as well as nominally pure crystals (waveguide 2). The latter is of particular interest because undoped LiNbO₃ wafers of several cm diameter, especially designed for waveguide fabrication and large enough for the realization of a practical device, are readily available. The aim is to coat only certain parts of the wafer with a thin layer of iron and to perform the indiffusion afterwards. This allows us to adjust the local impurity concentration and to tailor the properties of an integrated device.

As a test, a 5-nm-thin layer of iron is indiffused for 93 h at 1030 °C on the top face of sample 2 where, afterwards, the waveguide layer is formed. Then, indiffusion of a 100-nm-thick titanium layer is performed at a temperature of 1000 °C for 36 h in an argon atmosphere. Waveguide 1a was fabricated by one single indiffusion step of 80-nm titanium for 14 h at 1000 °C.

Figure 1 shows the calculated distributions of iron and titanium in sample 2. Gaussian-shaped curves are obtained, if we assume a diffusion process with an exhaustive source [5]. The iron concentration is almost constant in the area of high titanium concentration defining the waveguide layer. On the other hand, the concentration of the indiffused iron finally

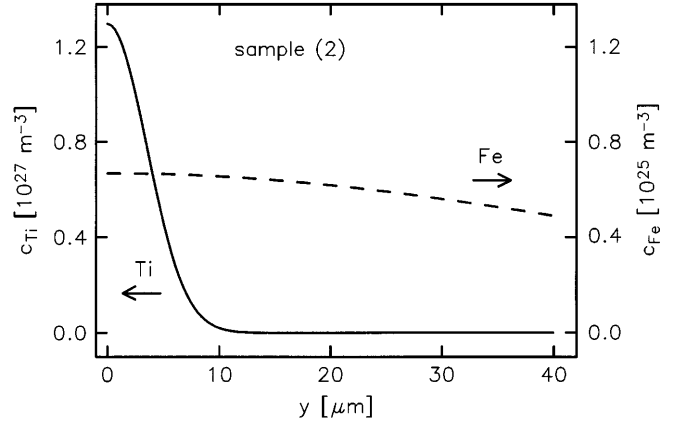


Fig. 1. Titanium and iron concentrations (c_{Ti} and c_{Fe}) of sample 2, calculated from diffusion theory. The parameter y denotes the distance from the surface of the waveguide

reaches zero in the bulk material. Consequently, the refractive index modulations induced by the electrooptic effect in the bulk part of sample 2 are expected to be rather low and hardly detectable.

The reduction state of the homogeneously iron-doped samples is determined by taking absorption measurements with a Cary 17D spectrometer. Then we use the proportionality relation of the Fe²⁺ concentration and light absorption in the blue wavelength region, $c_{\text{Fe}^{2+}} = \alpha_{477 \text{ nm}} \times 2.16 \times 10^{21} \text{ m}^{-2}$ [6]. Light propagation during the absorption measurements is always perpendicular to the waveguide layer, thus only an averaged absorption coefficient for the whole sample, including waveguide layer and substrate material, can be given. Therefore, this method can only be used for homogeneously doped samples. The proton concentration c_{H^+} , being of crucial importance for thermal fixing, is determined by absorption measurements as well, via a Fourier spectrometer and the relation $c_{\text{H}^+} = \alpha_{2.8 \mu\text{m}} \times 1.66 \times 10^{22} \text{ m}^{-2}$ [7]. However, the restrictions mentioned before also apply.

All waveguides are investigated by means of dark-mode spectroscopy in order to determine the effective refractive indices $n_{\text{eff},i}$ of the guided TE_{*i*} modes at $\lambda = 632.8 \text{ nm}$. Each refractive index profile $\delta n_e(y)$ is reconstructed by using an improved inverse WKB formalism [8]. With the help of this data the effective propagation depth d_{eff} of a TE mode can be calculated by a numerical integration of the mode equations (3,4) and the use of (5).

After complete experimental investigation, sample 1a is then annealed for 24 h at 1000 °C in oxygen to diminish the refractive index profile. The modified waveguide is denoted by 'sample 1b'. Its reduction state (Fe²⁺/Fe³⁺) is adjusted to nearly that of sample 1a by performing a short annealing treatment in an argon atmosphere at 1025 °C. We also check the proton concentration before and after annealing and find an increase by a factor of about four (see Table 1). Figure 2 shows the two reconstructed refractive index profiles for TE modes. Their effective depths d_{eff} at $\lambda = 632.8 \text{ nm}$ are indicated by vertical lines. Note that during the annealing treatment the index profile is strongly diminished. From the surface values $\delta n_e(y=0)$ extracted from the reconstructed profiles and data of [5] we derive a titanium concentration at the surface of $c_{\text{Ti}}(y=0) = 0.9 \times 10^{27} \text{ m}^{-3}$ after annealing com-

Table 1. Fabrication parameters of the investigated waveguides on *y*-cut LiNbO₃ substrates. The surface concentration $c_{\text{Ti}}(0)$ is deduced from the measured refractive index profiles. The ratio $c_{\text{Fe}^{2+}}/c_{\text{Fe}^{3+}}$ of Fe²⁺ and Fe³⁺ ions and the proton concentration c_{H^+} are extracted from absorption measurements

Waveguide	$c_{\text{Ti}}(0)$ 10^{27} m^{-3}	$c_{\text{Fe}^{2+}}/c_{\text{Fe}^{3+}}$	c_{H^+} 10^{23} m^{-3}
1a	1.7	0.13	2.0
1b	0.9	0.12	8.1
2	1.6	?	?

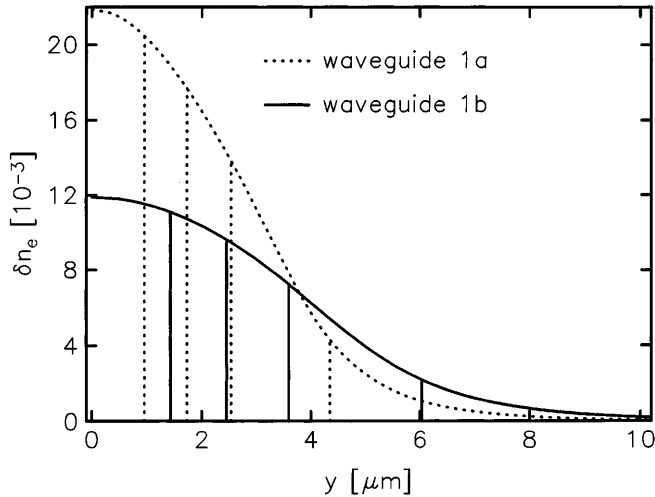


Fig. 2. The refractive index profile $\delta n_e(y)$ before (waveguide 1a) and after additional annealing (waveguide 1b) versus depth y . Vertical lines indicate the effective propagation depths of TE modes at $\lambda = 632.8 \text{ nm}$

pared to an initial value of $c_{\text{Ti}}(y=0) = 1.7 \times 10^{27} \text{ m}^{-3}$. For waveguide 2 the profile reconstruction yields $c_{\text{Ti}}(y=0) = 1.6 \times 10^{27} \text{ m}^{-3}$, which is about 20% larger than the surface value of $1.3 \times 10^{27} \text{ m}^{-3}$ (see Fig. 1) derived from diffusion theory. The data set characterizing the fabricated waveguides is summarized in Table 1.

2.2 Holographic measurements

A two-beam interference setup is used to record phase gratings in the waveguides. The experimental scheme is shown in Fig. 3a. The two writing beams I_S and I_R are expanded

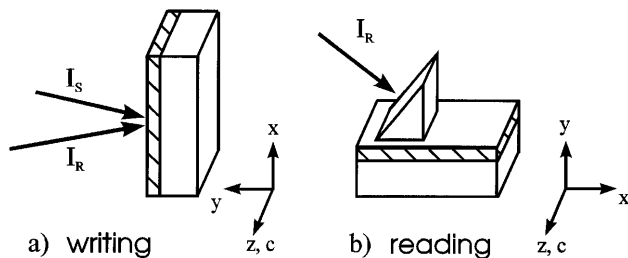


Fig. 3a,b. Geometry of the waveguide for hologram writing and reading. **a** Two expanded writing beams I_S, I_R of extraordinary polarization illuminate the whole sample. **b** Gratings are read using guided TE modes excited via a rutile prism

by suitable lenses and illuminate the whole sample with the waveguide layer on its top face. The light polarization is chosen to be along the *c* direction. Note that the two beams impinge upon the sample in a plane of incidence that is perpendicular to the waveguide layer. In all our recording experiments we use the light of an argon ion laser at $\lambda = 514.5 \text{ nm}$. The two writing beams intersect at an angle of $2\theta = 20^\circ$ (in air), which results in a grating period of $\Lambda = 1.5 \mu\text{m}$ in the waveguide. Each beam has an intensity of 240 Wm^{-2} . All fixing experiments are performed in the following way. First, the sample is heated with the help of a Eurotherm controller to a temperature of $180 \pm 0.1^\circ \text{C}$. Then, the two writing beams are switched on and the grating is written. After the beams are switched off, the waveguide is cooled down, and the fixed grating is developed with the white light of a halogen lamp. Elementary holograms recorded in this way are called ‘fixed gratings, recorded at 180°C ’ throughout this paper. Unfixed holographic gratings are recorded by using the same writing geometry, except that the sample is kept at a temperature of about 20°C . In the following they are labelled as ‘unfixed gratings written at room temperature’.

For readout of the recorded gratings a weak laser beam of a He–Ne laser with a wavelength of $\lambda = 632.8 \text{ nm}$ is coupled into the waveguide via a rutile prism, as illustrated in Fig. 3b. The various TE modes are excited by adjusting the coupling angle. Because of the small dimensions of the samples, $x_0 \times y_0 \times z_0 \approx 3 \text{ mm} \times 1 \text{ mm} \times 5 \text{ mm}$, we cannot apply an out-coupling prism, and the transmitted and the diffracted beam both leave the waveguide via the polished endface. A cylindrical lens focuses the outcoupled light onto photodetectors. For the homogeneously iron-doped samples, we are able to determine accurately the distance s that the light has travelled in the waveguide when the hologram is read: we measure the diffraction efficiency η of the bulk material in both the writing and the readout geometry. Knowing the thickness y_0 of our crystals, we can calculate the interaction length s by using Kogelnik’s formula. For waveguide 2 this is not possible because it is inhomogeneously doped with iron, and s can only be approximated by the distance between the incoupling spot at the prism and the endface of the sample.

2.3 Active phase stabilization system

To fix a hologram efficiently, it is essential that the crystal is heated to high temperatures during recording. Large temperature gradients are generated, which crucially affect the stability of the setup because of air convection and thermal expansion. This results in a distortion of the phase relation between the two writing beams; the phase relation being almost random. Consequently, the interference pattern in the sample begins to move and the modulation of the fixed grating is rather small. Performing the whole fixing experiment in a vacuum chamber [9] is one way of suppressing this effect. An alternative is the implementation of an active stabilization system [10–12]. Our experimental setup is illustrated schematically in Fig. 4. One of the writing beams is phase-modulated with the help of a piezo-driven mirror. We denote the modulation signal by $\psi_d \sin(\Omega t)$, where ψ_d is the amplitude and Ω the frequency. A small glass plate is placed directly behind the waveguide. This plate is lifted slightly, so that light can impinge upon it without traveling through the

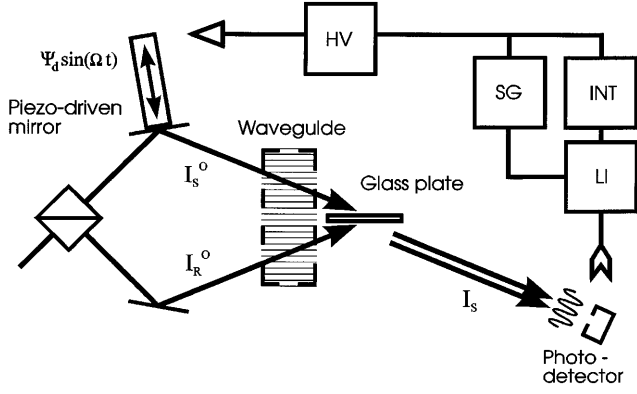


Fig. 4. The holographic setup and the active stabilization system. A small glass plate yields a second interference pattern that is imaged on a photodetector. HV, high-voltage amplifier; SG, sine-generator; LI, lock-in amplifier; INT, integrator

crystal. If the plate is properly adjusted, one writing beam is partly reflected from the plate, precisely in the direction of the other beam. A second interference pattern appears and this is imaged on a photodetector. The detector carries a small iris diaphragm, its diameter being small compared to the period of the intensity pattern. A lock-in amplifier, tuned to Ω , separates the control signal I^Ω , by which the active stabilization system is driven [10]:

$$I^\Omega = -2\sqrt{I_S^0 I_R^0} \psi_d \sin([k_S - k_R] \cdot \mathbf{r} + \psi) \sin(\Omega t). \quad (9)$$

In this equation k_S and k_R denote the wavevectors, and ψ is the general phase difference between the writing beams. The signal I^Ω is integrated and fed together with $\psi_d \sin(\Omega t)$ to a high-voltage amplifier that drives the piezo crystal. The performance of the stabilization system is as follows. Each time a perturbation occurs, the control signal I^Ω acquires a non-zero value. The piezo crystal starts to move until the control signal has vanished again. As a result, the phase relation ψ will be preserved.

3 Experimental results

Figure 5 shows the depth dependence of the refractive index modulation of a thermally fixed grating in the waveguide layer of sample 1a recorded for 120 min at 180 °C. The grating is read with light of different laser lines between 457 nm and 690 nm in order to increase the number of measured values for $\langle \Delta n_{\text{fix}} \rangle$. It can be concluded that thermal fixing works not only in bulk LiNbO₃:Fe crystals, but also in LiNbO₃:Fe:Ti waveguides. The modulation $\langle \Delta n_{\text{fix}} \rangle$ is not constant over the waveguide layer. The closer we come to the surface of the waveguide, the lower are the observed values $\langle \Delta n_{\text{fix}} \rangle$. The solid line indicates a fit of a Gaussian function with a constant width corresponding to that of the refractive index profile. As the profile $\delta n_e(y)$ is a measure for the distribution of titanium ions in the waveguide [5], we conclude that there is a strong correlation between the titanium concentration c_{Ti} and the inverse refractive index modulation $\langle \Delta n_{\text{fix}} \rangle$.

In Fig. 6 the results of recording unfixed holograms at room temperature in the same waveguide 1a are presented for different writing times. The refractive index modulations

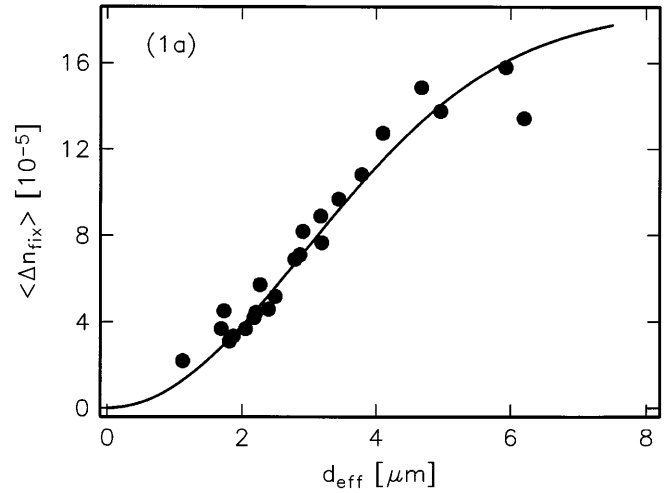


Fig. 5. Refractive index modulation $\langle \Delta n_{\text{fix}} \rangle$ of a grating written and fixed simultaneously at 180 °C for 120 min in waveguide 1a as a function of effective depth d_{eff} . The solid line is the best fitting Gaussian function; its width coincides with that of the reconstructed refractive index profile

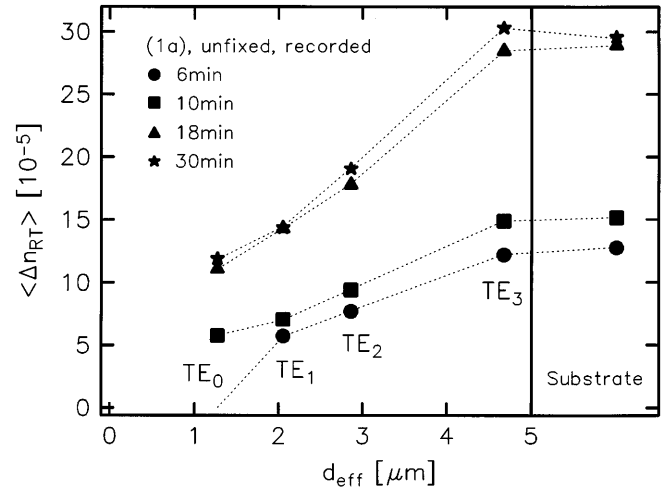


Fig. 6. Refractive index modulation $\langle \Delta n_{\text{RT}} \rangle$ of unfixed gratings recorded at room temperature in waveguide 1a as a function of effective depth d_{eff}

measured in the bulk material are shown in the right-hand part of the figure. We see the tendency for a strong lowering of the modulation $\langle \Delta n_{\text{RT}} \rangle$ at the top of the waveguide layer for these unfixed gratings. Even an increase in the recording time of up to 30 min cannot suppress this effect.

In Fig. 7 we illustrate the refractive index changes of fixed gratings for different writing times in sample 1a. Large amplitudes for TE modes guided deep in the sample are measured, and these increase with recording time. In contrast to these results, the absolute values for the TE₀ mode near the surface remain at a low level, often hardly detectable.

Then we repeat the experimental investigation with waveguide 1b. Again, unfixed gratings are written at room temperature and compared with fixed gratings recorded at 180 °C. From the results obtained with unfixed gratings, shown in Fig. 8, it can be concluded that the annealing treatment affects writing even at room temperature. A decrease in the refractive index modulation near the surface is still

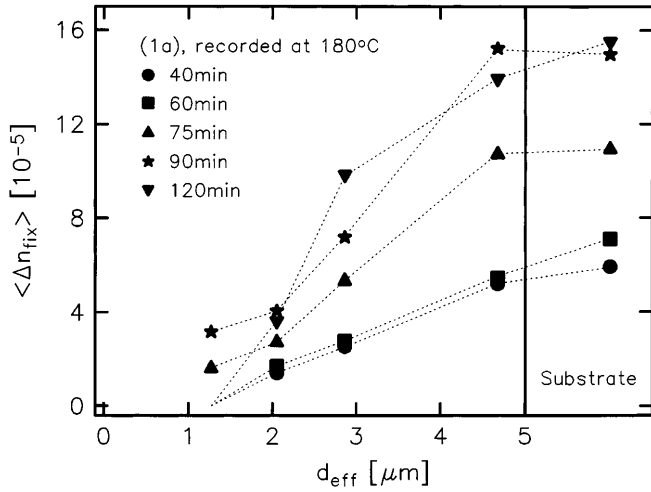


Fig. 7. Refractive index modulation ($\langle \Delta n_{\text{fix}} \rangle$) observed for thermally fixed gratings recorded at 180 °C in waveguide 1a as a function of effective depth d_{eff}

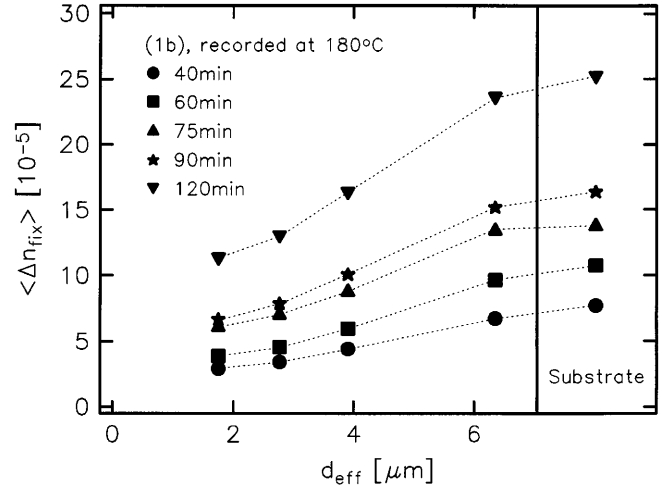


Fig. 9. Refractive index modulation ($\langle \Delta n_{\text{fix}} \rangle$) of thermally fixed gratings recorded at 180 °C in waveguide 1b as a function of effective depth d_{eff} . Relatively high values are measured over the whole waveguide layer, even for the TE_0 mode

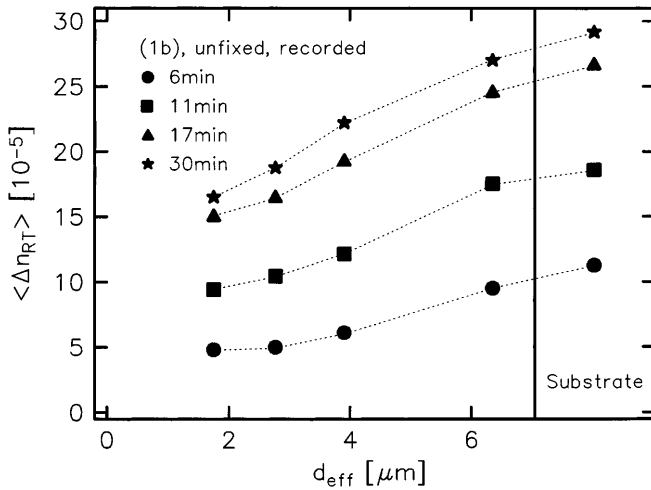


Fig. 8. Refractive index modulation ($\langle \Delta n_{\text{RT}} \rangle$) of unfixed gratings written at room temperature in waveguide 1b as a function of effective depth d_{eff}

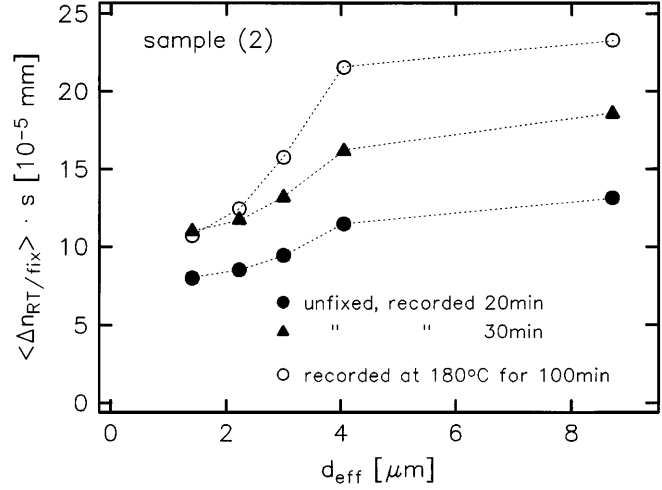


Fig. 10. Refractive index modulations ($\langle \Delta n_{\text{fix}} \rangle$) and ($\langle \Delta n_{\text{RT}} \rangle$) of a grating written and fixed at 180 °C and of two unfixed gratings recorded at room temperature in waveguide 2 as a function of effective depth d_{eff} . Here, the measurement of Δn_{fix} and Δn_{RT} in the substrate is not possible. For this reason the interaction length s cannot be derived precisely

present, but the values for the substrate and the TE_0 mode differ much less than in waveguide 1a.

Figure 9 shows the results for fixed holograms recorded at 180 °C in sample 1b. Comparison of Fig. 9 and Fig. 7 leads to the conclusion that thermal fixing works much better after the thermal treatment. As the writing time is increased the measured refractive index modulation of fixed gratings still increases over the whole waveguide layer. Even for the TE_0 mode, a modulation of ($\langle \Delta n_{\text{fix}} \rangle \approx 1 \times 10^{-4}$) is observed.

We investigated fixed, as well as unfixed gratings recorded at room temperature in the double-diffused waveguide 2. Here the observed modulations ($\langle \Delta n_{\text{RT}} \rangle$) and ($\langle \Delta n_{\text{fix}} \rangle$), of unfixed and fixed gratings, are shown together in Fig. 10. Thermal fixing works in the waveguide layer of sample 2, too. As already pointed out, the distance s that the reading beam has travelled through this waveguide is not exactly known, but the assumption of $0.7 \text{ mm} < s < 1.3 \text{ mm}$ seems to be quite

reasonable. Again, the decrease in the measured refractive index modulations in the surface area is obvious. This holds for thermally fixed gratings as well as for gratings written at room temperature.

4 Discussion

We want to give a possible explanation for the decrease in the measured refractive index modulations near the surface of the waveguides investigated. Several authors have proposed a model in which one assumes stabilization of Fe^{2+} by the indiffused titanium [4, 13] found in LiNbO_3 only in the valence state Ti^{4+} . This effect is especially pronounced for large titanium concentrations. The titanium concentration reaches values of about 10^{27} m^{-3} in the surface region of our waveguides. However, the typical iron concentration of the sam-

ples is much lower; we estimate values of 10^{25} m^{-3} . So we suppose that the $\text{Fe}^{2+}/\text{Fe}^{3+}$ ratio of our samples decreases with increasing depth of the waveguiding layer.

For $\text{LiNbO}_3:\text{Fe}$ bulk crystals the relation $\Delta n_s \sim c_{\text{Fe}^{3+}}$ is well established [14], with Δn_s as the saturation value of the refractive index modulation of a holographic grating written at room temperature. This agrees with our measured data: the values $\langle \Delta n_{\text{RT}} \rangle$ of the refractive index modulation decrease in the region of high titanium concentration where the Fe^{3+} concentration decreases.

We could not prove unambiguously whether protons are the charge-compensating ions during thermal fixing in our investigated waveguides, or whether other positively charged ions are involved, too. This is mainly because the proton concentration in the waveguide layer itself cannot be measured precisely. There are some hints that protons participate in the process: during additional annealing of waveguide 1a, the proton concentration increases by a factor of four. It can be deduced from Figs. 7 and 9 that fixing in the substrate of this guide works better with increased proton concentration and leads to larger index changes. This effect is even more pronounced in the waveguide layer, but could probably be caused by the strong decrease in the local titanium concentration as well. Unfortunately, we cannot separate these two effects.

5 Conclusions

In summary, thermal fixing of holographic gratings in planar titanium-indiffused LiNbO_3 waveguides was demonstrated. We observed large refractive index modulations of fixed phase gratings that are comparable with those obtained in the bulk material. Simultaneously, we observed a more or less

pronounced decrease in the measured modulations for the TE modes guided near to the surface. The large titanium concentration is assumed to be responsible for this effect. As a consequence, one should adjust the refractive index profile of a $\text{LiNbO}_3:\text{Ti}$ waveguide to be rather low, in order to ensure a nearly constant modulation of fixed gratings over the whole waveguide layer. Nevertheless, the obtained modulations of thermally fixed gratings in LiNbO_3 waveguides are high enough to allow devices in integrated optics to be realized.

Acknowledgements. Financial support of the Deutsche Forschungsgemeinschaft (SFB 225, D9) is gratefully acknowledged.

References

1. J.J. Amodei, D.L. Staebler: Appl. Phys. Lett. **18**, 540 (1971)
2. H. Vormann, G. Weber, S. Kapphan, E. Krätzig: Solid State Commun. **40**, 543 (1981)
3. H. Kogelnik: Bell. Syst. Tech. J. **48**, 2909 (1969)
4. V. Gericke, P. Hertel, E. Krätzig, J.P. Nisius, R. Sommerfeldt: Appl. Phys. B **44**, 155 (1987)
5. J. Vollmer, J.P. Nisius, P. Hertel, E. Krätzig: Appl. Phys. A **32**, 125 (1983)
6. H. Kurz, E. Krätzig, W. Keune, H. Engelmann, U. Gonser, B. Dischler, A. Räuber: Appl. Phys. **12**, 355 (1977)
7. S. Kapphan, A. Breitkopf: Phys. Stat. Sol. (a) **133**, 159 (1992)
8. P. Hertel, H.P. Menzler: Appl. Phys. B **44**, 75 (1987)
9. L. Arizmendi, P.D. Townsend, M. Carrascosa, J. Baquedano, J.M. Cabrera: J. Phys: Condens. Matter **3**, 5399 (1991)
10. A.A. Freschi, J. Frejlich: Opt. Lett. **20**, 635 (1995)
11. J. Frejlich, P.M. Garcia, A.A. Freschi: Opt. Mat. **4**, 410 (1995)
12. J. Frejlich, L. Cescato, G.F. Mendes: Appl. Opt. **27**, 1967 (1988)
13. A.M. Glass, I.P. Kaminov, A.A. Ballman, D.H. Olson: Appl. Opt. **19**, 276 (1980)
14. E. Krätzig, H. Kurz: Opt. Acta **24**, 475 (1977)